doi: 10.59429/ace.v8i3.5707

ORIGINAL RESEARCH ARTICLE

Multi-cycle regeneration of cation and anion exchange resins in a continuous-flow water treatment system

Thulfuqar A. Jawad*, Sata K. Ahmed Ajjam

Chemical engineering department, Collage of engineering, Babylon university, Babylon City, 51002, Iraq

*Corresponding author: Thulfugar A. Jawad, thulfugar.jawad.engh430@student.uobabylon.edu.iq

ABSTRACT

This study evaluates the regeneration performance and long-term operability of a continuous-flow, dual fixed-bed ion-exchange system for the simultaneous removal of lead (Pb²⁺) and nitrate (NO₃⁻) from water. Two acrylic columns (total height 45 cm; internal diameter 3.0 cm), each packed with 40 g of resin, were operated in series at pH 7.0 ± 0.1 : a strong-acid cation exchanger (Purelite C100) for Pb2+ and a strong-base anion exchanger (ResinexTM NR-1) for NO₃-. Packed-bed heights were 8.0 cm (≈56.6 mL) for the cation column and 9.0 cm (≈63.6 mL) for the anion column. A 12run Box-Behnken design investigated inlet concentration (40-80 mg L⁻¹), temperature (25-60 °C), and flow rate (40-100 mL min⁻¹) before and after regeneration with 10% (w/w) NaCl. Under optimized conditions (≈43 °C; 60 mL min⁻¹; 40 mg L⁻¹), Cycle 1 removals were 82.5% (Pb²⁺) and 92.3% (NO₃⁻). After six regeneration cycles, removals declined moderately to 70.2% and 83.6%, respectively, indicating good reusability with a slower efficiency decay for the anion resin. Quadratic response-surface models fit the data well (adjusted R² = 0.973 for Pb²⁺; 0.999 for NO₃⁻); concentration and flow were dominant negative factors, while elevated temperature mitigated mass-transfer limitations. A 10% NaCl protocol is therefore an effective baseline for routine regeneration, with scope for further capacity retention via longer brine contact, occasional deep-clean steps, or tailored regenerant dosing.

Keywords: regeneration of resin; ion exchange; lead removal; nitrate removal; purelite C100 resin regeneration; resinexTM NR-1 resin regeneration; water purification; continuous flow

ARTICLE INFO

Received: 21 July 2025 Accepted: 20 August 2025 Available online: 26 August 2025

COPYRIGHT

Copyright © 2025 by author(s). Applied Chemical Engineering is published by Arts and Science Press Pte. Ltd. This work is licensed under the Creative Commons Attribution-NonCommercial 4.0 International License (CC BY 4.0). https://creativecommons.org/licenses/by/4.0/

1. Introduction

Ion exchange (IX) is a widely used water treatment technology that replaces unwanted ions in water with more desirable ones using synthetic resins. It is efficient, adaptable, and cost-effective, making it essential for removing contaminants like nitrates, lead, and hardness ions in both industrial and municipal systems^[1,2].

ISSN: 2578-2010 (O)

Ion exchange sustainability relies on effective resin regeneration, as resins lose capacity when saturated with exchanged ions. Regeneration typically using strong acids for cation resins and strong bases for anion resins restores performance, extends resin lifespan, lowers costs, and reduces environmental impact^[3,4].

Stricter environmental regulations and growing water scarcity have heightened the emphasis on sustainable treatment practices. Regeneration efficiency is now a critical metric, affecting resin lifespan, water quality, and chemical waste generation. While conventional methods are effective, they often require high chemical inputs and produce substantial brine waste, driving the development of innovative

approaches that reduce chemical use, recycle regenerants, and enhance overall sustainability^[5,6].

Recent advances in ion exchange technology include selective resin formulations, alternative regenerants, and techniques like counter-current regeneration and low-concentration dosing. These innovations enhance regeneration efficiency and environmental compatibility, positioning resin regeneration as a vital element of system design and performance optimization rather than merely routine maintenance^[7,8].

This study presents the fundamental principles and mechanisms of ion exchange resin regeneration, emphasizing its impact on operational longevity, economic viability, and environmental compliance. By reviewing conventional methods alongside emerging innovations, it establishes a foundation for evaluating regeneration strategies in both experimental and practical water treatment contexts.

2. Principles of ion exchange and regeneration

Understanding the functional group chemistry of ion exchange resins is essential for optimizing their performance in water treatment systems. The efficiency of ion exchange is largely determined by the type, density, and chemical stability of the resin's active sites. In this study, two resins were utilized: Purelite C100, a strong acid cation resin, and Resinex NR-1, a strong base anion resin, each containing distinct functional groups that facilitate the exchange of cations or anions in aqueous solutions^[9,10].

2.1. Purelite C100 cation exchange resin

Pure lite C100 is a gel-type strong acid cation exchange resin composed of a cross-linked polystyrene-divinylbenzene (PS-DVB) matrix functionalized with sulfonic acid groups (–SO₃H). These sulfonic groups are highly ionized in solution, regardless of pH, making them extremely effective for cation exchange under a wide range of conditions from acidic to neutral and mildly basic environments^[11]. **Table 1** Show Purelite C100 properties.

Operation reaction is: - $2 R - SO_3^-Na^+ + Pb^{2+} \rightleftharpoons (R - SO_3^-)_2 Pb^{+2} + 2 Na^+ \qquad(eq.1)$ Regeneration reaction: - $(R - SO_3^-)_2 Pb + 2 Na^+ \rightleftharpoons 2 R - SO_3^-Na^+ + Pb^{2+} \qquad(eq.2)$

Table 1. Purelite C100 properties.

Structure of Polymers	Divinylbenzene crosslinked gel polystyrene		
Appearance	Sphere-shaped beads		
Functional Group	Sulfonic Acid		
Ionic Form	Na ⁺ form		
Total Capacity (min.)	2.0 eq/L (43.7 Kgr/ft³) (Na ⁺ form)		
Moisture Retention	44 to 48 %		
Specific Gravity	1.29		
Range of Particle Size	300 - 1200 μm		
Temperature Limit	120 °C (248.0 °F)		
Reversible Swelling, Na \rightarrow H (max.)	9 %		
Uniformity Coefficient (max.)	1.7		

Table 1 show the properties of Purelite C100 is a strong-acid cation-exchange resin made from divinylbenzene-crosslinked polystyrene and supplied in the Na⁺ form as small spherical beads (300–1200 μ m, uniformity coefficient \leq 1.7). It has a total capacity \geq 2.0 eq/L, moisture retention of 44–48%, specific gravity of \sim 1.29, and a maximum operating temperature of 120 °C, with reversible swelling \leq 9% during Na \leftrightarrow H

cycling. The high density and strong acidity of its sulfonic groups provide fast ion-exchange kinetics and high capacity, making the resin well suited for water softening, heavy-metal (e.g., Pb²⁺) removal, and industrial demineralization^[12].

2.2. Resinex NR-1 anion exchange resin

Resinex NR-1 is a strong base anion exchange resin based on a similar PS-DVB structure, but functionalized with quaternary ammonium groups (-N⁺(CH₃) ₃Cl⁻). These groups are permanently ionized and capable of exchanging a broad spectrum of anions over the entire pH scale^[13]. **Table 2** Show the properties of ResinexTMNR-1.

Table 2. ResinexTMNR-1 chemical and physical features^[14].

Resinex TM NR-1 Chemical and Physical Features			
Type Crosslinked	polystyrene divinylbenzene		
Form microporous	milky white, spherical beads		
Functional group	Quaternary amine, Type 1		
Whole bead	count 95% min.		
Ionic form, as shipped	Cl-		
Bead size	0.42 - 1.25 mm		
Uniformity coefficient	1.60 max.		
Bulk density, as shipped	680 kg/m3		
Real density	1.08 g/cm3		
Water retention	50 - 60%		
Total capacity (Cl- form).	1.15 eq/l min		
Volume change Cl> OH-	20% max.		
Stability, pH	0 - 14		

ResinexTM NR-1 is a strong-base anion-exchange resin of crosslinked polystyrene—divinylbenzene, supplied as milky-white, spherical, microporous beads in the Cl⁻ form (\geq 95% whole beads). It uses Type-I quaternary ammonium functional groups, remains stable across pH 0–14, and shows a total capacity \geq 1.15 eq/L (Cl⁻ form). Bead size is 0.42–1.25 mm with a uniformity coefficient \leq 1.60; water retention is 50–60%, bulk density \sim 680 kg/m³, and true density \sim 1.08 g/cm³. The resin exhibits \leq 20% reversible volume change on Cl⁻ \rightarrow OH⁻ conversion. High selectivity of the quaternary ammonium sites for nitrate and related oxyanions enables efficient removal in drinking-water treatment, with strong-base character ensuring sustained ionization and rapid exchange under neutral to alkaline conditions^[14].

Exchange Reaction (example):

$$R-N^+(CH_3) \circ Cl^- + NO_3^- \rightleftharpoons R-N^+(CH_3) \circ NO_3^- + Cl^-$$
(eq.3)

Regeneration Reaction:

$$R-N^+(CH_3) \ 3 \ NO_3^- + CI^- \rightleftharpoons R-N^+(CH_3) \ 3 \ CI^- + NO_3^-$$
 (eq.4)

2.3. Selectivity coefficients of ion exchange resins

The performance of ion exchange resins in multi-ion systems is largely governed by selectivity coefficients, which quantify the resin's relative preference for exchanging one ion over another. These coefficients are influenced by factors such as ionic charge, hydrated radius, resin type, and solution conditions (e.g., pH, ionic strength). A higher selectivity coefficient indicates a stronger affinity of the resin for a specific ion, affecting both the order of ion removal and the difficulty of regeneration^[15].

Pure lite C100, a strong-acid cation-exchange resin, follows the selectivity sequence $Pb^{2+} \gg Ca^{2+} > Mg^{2+} > Na^+$, indicating a markedly stronger affinity for divalent and especially heavy-metal cations than for monovalent sodium. This preference arises from the higher charge density and strong electrostatic interaction of Pb^{2+} with the resin's sulfonate $(-SO_3^-)$ groups, enabling Pb^{2+} to displace Na^+ , Mg^{2+} , or even Ca^{2+} at low concentrations. The result is excellent performance for lead removal from contaminated water, with the practical implication that robust regeneration conditions are required to reverse Pb^{2+} loading and maintain long-term capacity^[11].

PureliteC100 strong affinity for divalent cations particularly Pb²⁺ complicates regeneration, as displacing tightly bound ions requires a high activity of competing Na⁺ supplied by concentrated NaCl brine; by mass action, the excess Na⁺ drives desorption and restores exchange sites. Sustained performance therefore depends on optimizing regenerant parameters (concentration, volume, contact time) to limit capacity fade. In contrast, ResinexTM NR-1 (strong-base, Type-I quaternary ammonium) follows a pronounced oxyanion selectivity sequence, $NO_3^- > SO_4^{2-} > HCO_3^- > Cl^-$. Its preference for nitrate arises from nitrate's relatively small hydrated radius and lower charge density, which facilitate rapid diffusion and stable binding. Regeneration of NR-1 typically employs NaOH, using a high OH⁻ concentration to reverse these affinities and elute adsorbed anions^[16].

Understanding selectivity coefficients is essential not only for predicting ion exchange behavior in complex water matrices but also for designing efficient regeneration strategies that extend resin life and minimize chemical use.

3. Regeneration methods

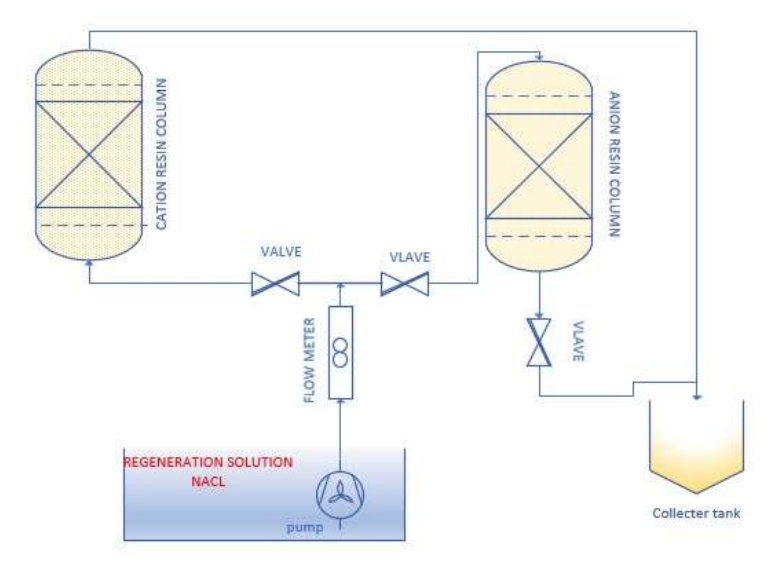


Figure 1. Regeneration process.

Effective regeneration of ion exchange resins is critical for restoring resin capacity, maintaining system performance, and extending operational lifespan. The choice of regeneration method depends on the resin type, system design, operational scale, and water quality. This section discusses key regeneration techniques, focusing on co-current and counter-current approaches, as well as batch versus continuous modes, highlighting modifications aimed at improving efficiency and sustainability^[17]. This study employes two types of regeneration as shown in **Figure 1**.

3.1. Modified co-current regeneration

Conventional co-current regeneration, where the regenerant flows in the same direction as the influent as shown in **Figure 2**, is simple but less efficient. Modifications such as partial bed regeneration and stepwise

regenerant addition improve contact efficiency. Using softened water during regeneration further enhances resin performance by preventing scaling, reducing regenerant losses, and prolonging resin life particularly for cation resins like Purelite C100. Overall, modified co-current regeneration offers a practical balance of simplicity, efficiency, and cost-effectiveness, making it well-suited for smaller systems or applications with limited process flexibility^[17,18].

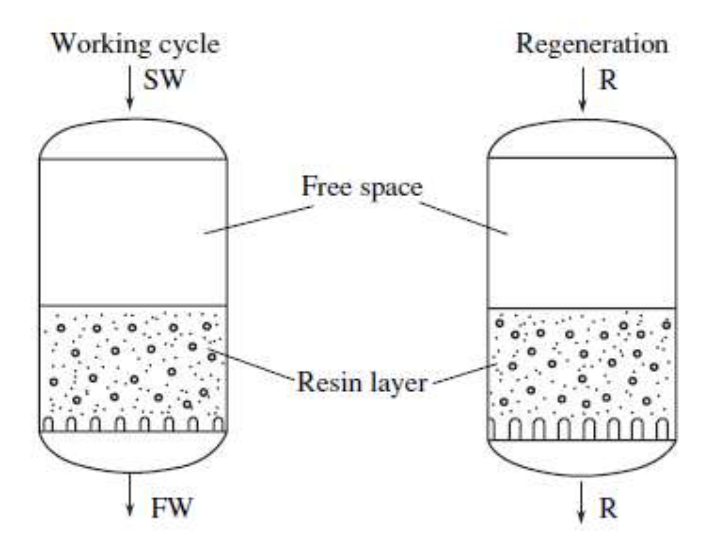


Figure 2. Schematic Co-Current Regeneration.

3.2. Counter-Current regeneration variants

Counter-current regeneration involves introducing the regenerant flow opposite to the service flow as shown in **Figure 3**. This method enhances regeneration efficiency by ensuring that the freshest regenerant contacts the most exhausted resin, resulting in more complete ion displacement and less regenerant waste.

Recent advancements include up flow packed-bed systems, where regenerant is introduced from the bottom of the resin bed moving upward. This orientation promotes better distribution, reduces channeling, and increases resin utilization. The improved contact between regenerant and resin beads yields higher throughput and lower salt usage compared to traditional downflow systems.

The counter-current approach is widely recognized for its superior regenerant efficiency and operational cost savings, especially in large-scale and continuous flow systems. It is often preferred in industrial applications targeting stringent water quality requirements^[19].

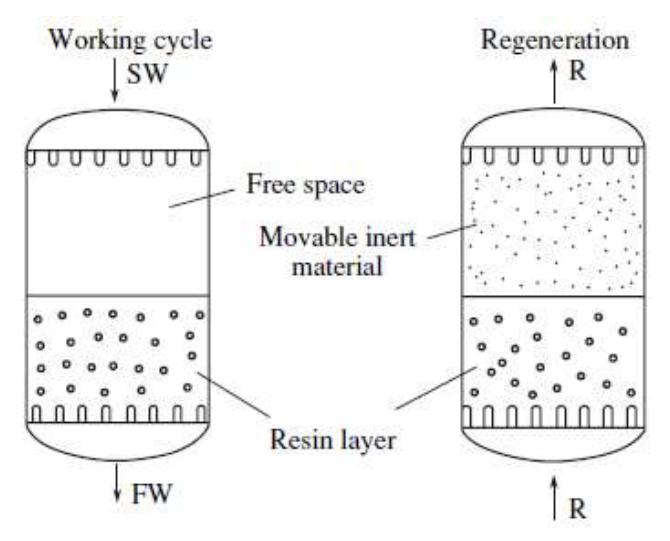


Figure 3. Counter-Current Regeneration.

3.3. Regeneration steps

The choice of 10% NaCl is supported by literature and industrial practice. Pure lite guidelines emphasize that achieving at least ~3% NaCl concentration within the resin beads requires an external brine concentration of around 10% to drive efficient ion displacement [23]. Similarly, Veolia's ion exchange handbook recommends 10% sodium chloride solution as the practical standard, noting that while higher dosages slightly increase capacity, the benefits plateau and lead to unnecessary chemical consumption [24]. Waterworld Magazine reports that 8–12% NaCl is typical for regeneration, with 10% being the norm, ensuring both efficiency and cost-effectiveness [25]. Finally, general references confirm that residential and industrial ion exchange systems commonly employ ~10% brine as an established regeneration standard [26].

Thus, 10% NaCl represents an optimal compromise: it provides sufficient regenerant strength to desorb multivalent cations such as Pb²⁺ and strongly bound anions like NO₃⁻, while avoiding excessive chemical use, minimizing operational costs, and reducing environmental impact. The regeneration steps shown in **Figure 4** below.

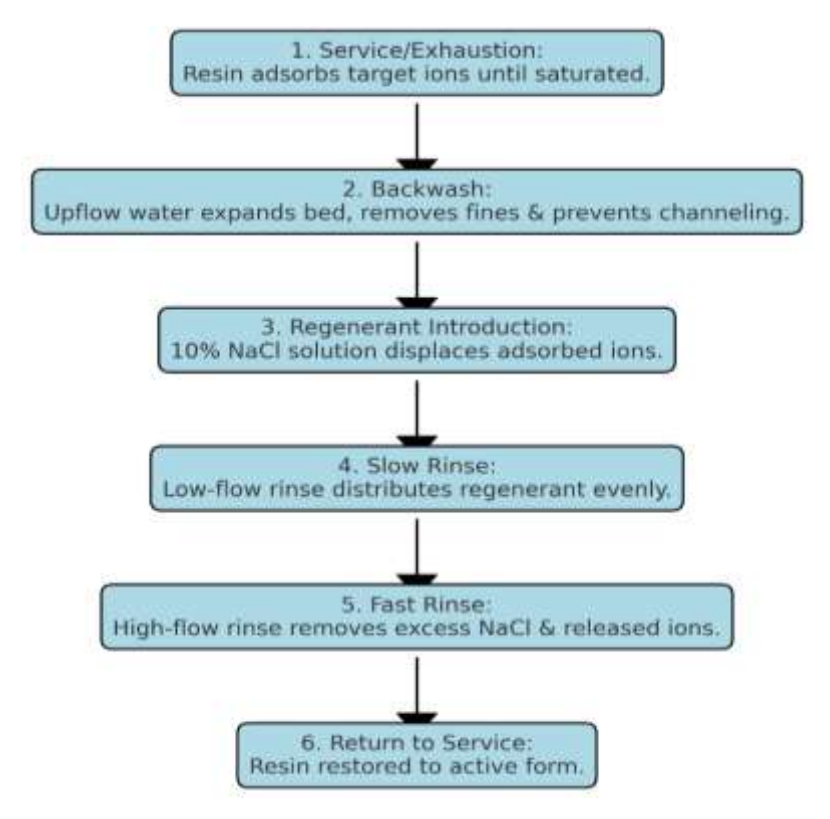


Figure 4. Schematic illustrates regeneration steps.

4. Results and discussion

A continuous ion-exchange system was used. The brine solution was preheated in a water bath, then pumped through a flowmeter into a cation-exchange column (Pure lite® C100) to regenerate and replace (Pb²+) with (Na+2). An anion-exchange column (ResinexTM NR-1) was also used to replace (NO₃⁻) with (Cl-). The experiment followed a Box–Behnken design with 12 runs, testing three variables—contaminant concentration (40, 60, 80 ppm), flow rate (40, 70, 100 mL/min), and temperature (25, 40, 60 °C)—at constant pH (7.1) and resin dose (40 g), as shown in **Table 3**. (Pb²+) concentrations were measured using an AA-7000 atomic absorption spectrophotometer (Shimadzu), and (NO3⁻) levels with a T60 UV-visible spectrophotometer (PG Instruments). As shown in **Table 3**, the removal efficiency was evaluated before and after the regeneration process.

Table 3. Displays the Box-Behnken design runs, along with the consequent elimination performance and the defined values for the operational variables.

				Before Re	generation	After Reg	generation
run	Initial Concentration	Temperature	Flow rate	NO3- Removal efficiency	Pb ⁺² Removal efficiency	NO3- Removal efficiency	Pb ⁺² Removal efficiency
	mg/l	C	ml/min	%	%	%	%
1	40	60	70	94.8	74.9	87.22	70.22
2	40	25	70	94	76.6	86.48	69.8
3	40	42.5	40	95.2	81.8	87.58	75.26
4	60	25	40	94.1	76.91	86.57	70.76
5	60	60	100	94.2	63.5	86.66	61.1
6	80	25	70	90.8	70.11	83.54	61.87
7	60	60	40	95.9	74.6	88.24	68.63
8	60	25	100	94	71.1	86.48	65.41
9	80	42.5	40	91.74	76.71	84.4	68.77
10	80	60	70	91.6	63.9	84.27	60.33
11	80	42.5	100	90.96	64.1	83.68	62.88
12	40	42.5	100	93.66	79.1	86.37	73.42

Table 3 (Box–Behnken design) summarizes how initial concentration (mg L⁻¹), temperature (°C), and flow rate (mL min⁻¹) affect removal of NO₃⁻ and Pb²⁺ before and after regeneration. NO₃⁻ removal remained consistently high typically ≥90% pre-regeneration with only minor declines post-regeneration. Pb²⁺ removal was more variable (≈63–82% pre-regeneration) and showed a more noticeable decrease after regeneration. Peak performances for both ions occurred at moderate feed concentrations and flow rates, indicating an interior optimum within the tested ranges rather than at extremes. The post-regeneration drops, especially for Pb²⁺, suggests partial capacity loss due to incomplete desorption of strongly bound species, underscoring the need to fine-tune regenerant strength, volume, and contact time to sustain long-term efficiency.

4.1. Effect of Operating Parameters on NO₃- Removal efficiency

4.1.1. Interaction effect between concentration and flow rate on NO₃⁻ removal

Figure 5 illustrates the interaction effect between initial concentration and flow rate on NO₃⁻ removal efficiency. The plot shows that at lower flow rates, NO₃⁻ removal remains high across different concentrations, indicating sufficient contact time for effective adsorption. However, as the flow rate increases, the removal efficiency tends to decrease, especially at higher concentrations. This suggests that higher flow rates reduce the residence time, limiting the interaction between the adsorbent and the contaminant. The figure highlights that optimal NO₃⁻ removal occurs at lower flow rates and moderate initial concentrations, emphasizing the importance of balancing these two parameters for maximum performance.

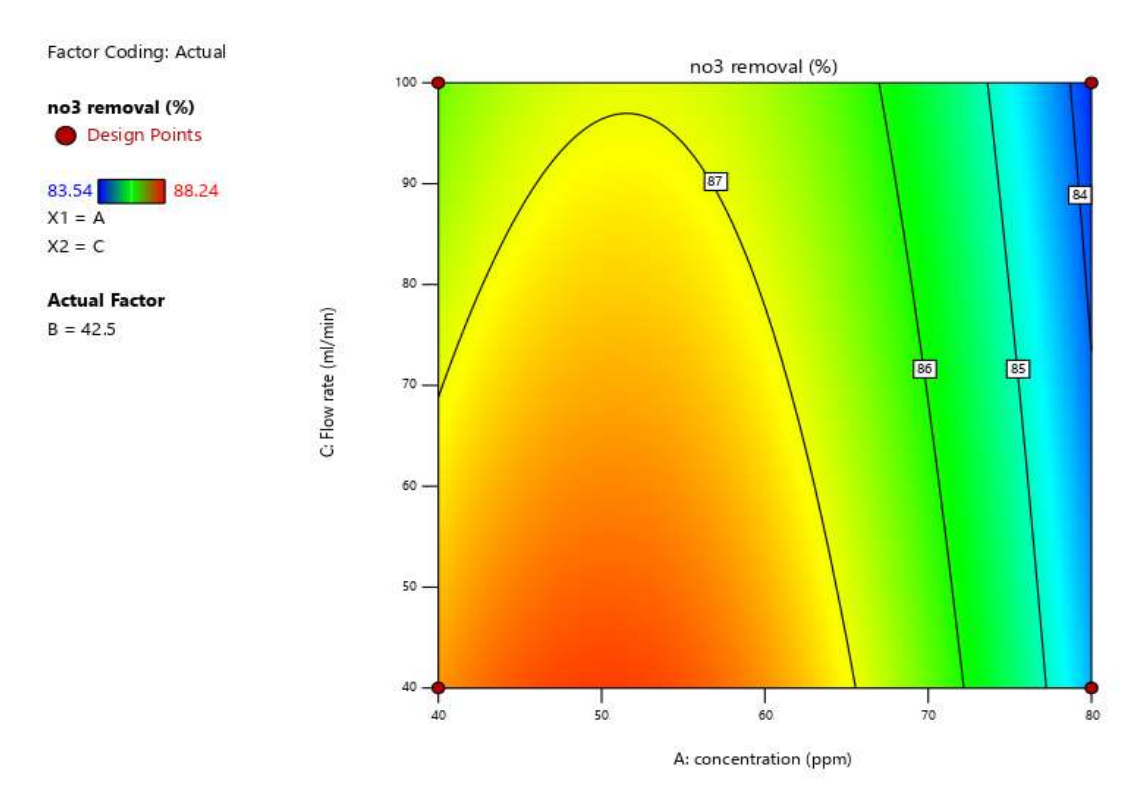


Figure 5. Interaction effect between concentration and flow rate on NO₃⁻ Removal.

4.1.2. Interaction effect between concentration and temperature on NO₃⁻ removal

Figure 6 demonstrates the interaction effect between initial concentration and temperature on NO₃⁻ removal efficiency. The figure indicates that at lower concentrations, temperature has a relatively minor effect on removal efficiency. However, at higher concentrations, increasing the temperature improves NO₃⁻ removal. This trend suggests that higher temperatures may enhance the diffusion rate of NO₃⁻ ions and increase the activity of the adsorbent surface. The interaction shows that the negative impact of high concentration can be partially offset by operating at elevated temperatures, highlighting the synergistic role of temperature in improving removal efficiency under higher pollutant loads.

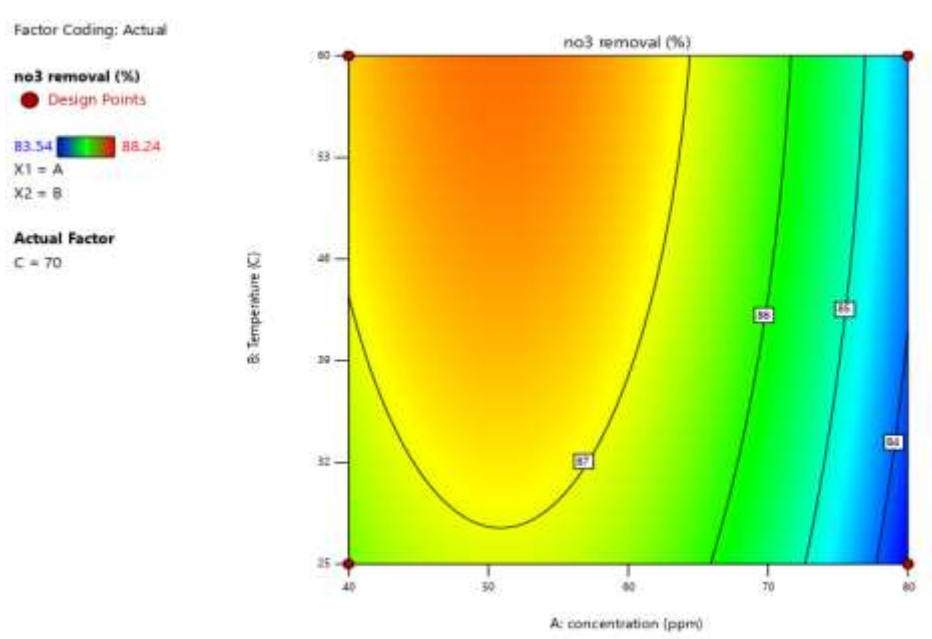


Figure 6. Interaction effect between concentration and temperature on NO₃⁻ Removal.

4.1.3. Interaction effect between flow rate and temperature on NO₃- Removal

Figure 7 illustrates the interaction effect between flow rate and temperature on NO₃⁻ removal efficiency. The results show that at lower flow rates, NO₃⁻ removal remains consistently high across different temperatures, indicating sufficient contact time for adsorption. However, as the flow rate increases, removal efficiency decreases, particularly at lower temperatures. This suggests that low temperatures combined with high flow rates negatively impact the adsorption process due to reduced ion mobility and limited interaction time. In contrast, higher temperatures help mitigate the negative effect of increased flow rate, likely by enhancing diffusion and adsorption kinetics. Overall, the figure highlights that optimal NO₃⁻ removal is achieved at high temperatures and low flow rates.

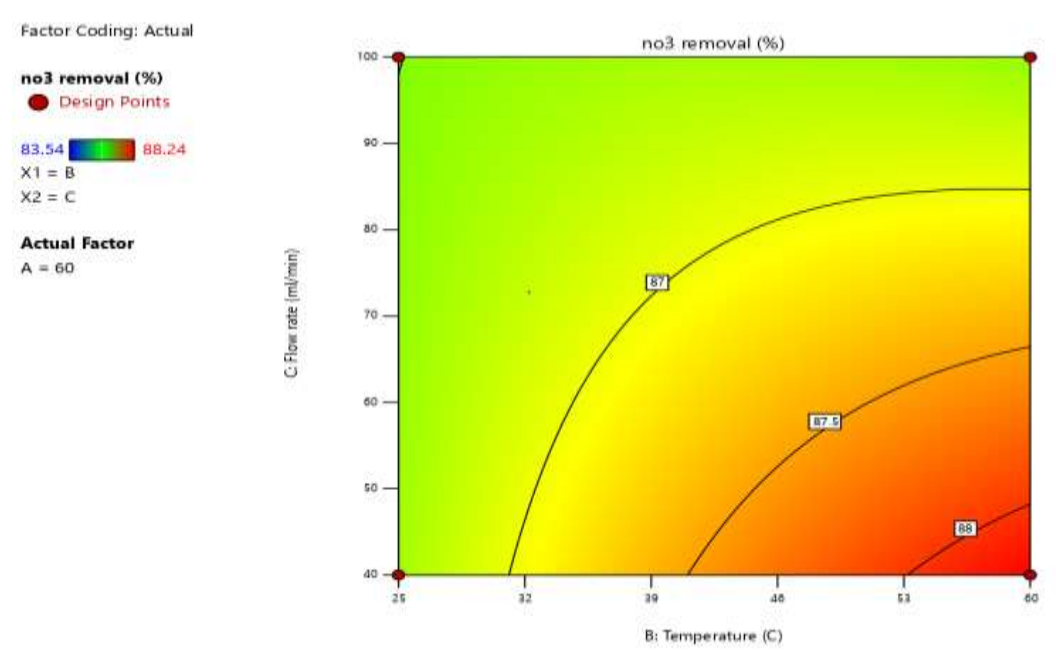


Figure 7. Interaction effect between flow rate and temperature on NO₃⁻ Removal.

4.1.4. Effect of concentration on NO₃⁻ removal after regeneration

Figure 8 shows the effect of initial concentration on NO₃⁻ removal efficiency after regeneration. The figure reveals a general decrease in removal efficiency as the concentration increases. At lower concentrations, the regenerated adsorbent maintains high removal performance, indicating sufficient active sites are still available. However, as concentration rises, the efficiency drops, suggesting that the regenerated material has a reduced adsorption capacity, possibly due to incomplete regeneration or saturation of adsorption sites. This trend highlights that after regeneration, the system performs better under lower contaminant loads, and its effectiveness declines with higher concentrations.

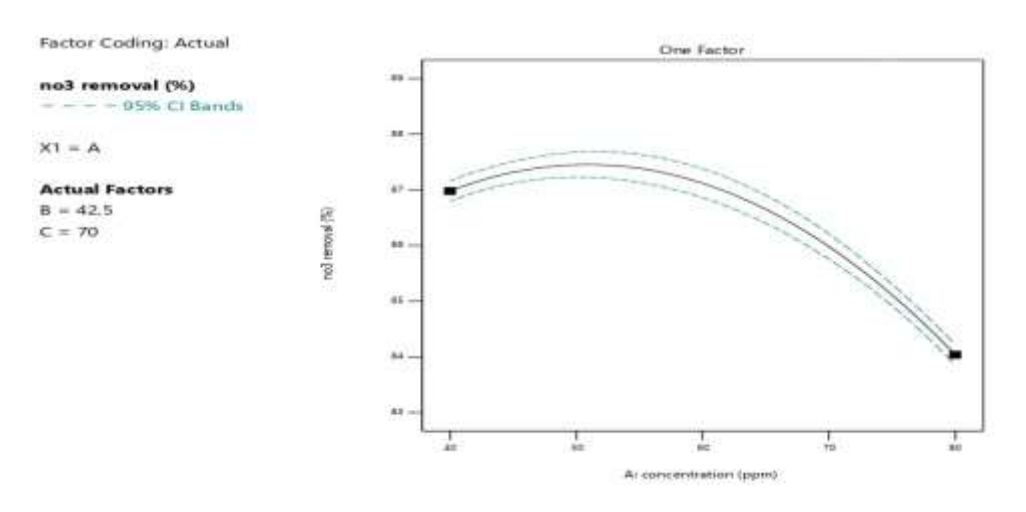


Figure 8. Effect of Concentration on NO₃⁻ Removal.

4.1.5. Effect of flow rate on NO₃- Removal after regeneration

Figure 9 illustrates the effect of flow rate on NO₃⁻ removal efficiency after regeneration. The data show that as the flow rate increases, the removal efficiency gradually decreases. At lower flow rates, the regenerated adsorbent performs more effectively, likely due to longer contact time between the solution and the adsorbent, allowing for better adsorption. In contrast, higher flow rates reduce the residence time, limiting the interaction and resulting in lower removal efficiency. This trend emphasizes the importance of maintaining controlled flow conditions after regeneration to maximize NO₃⁻ removal performance.

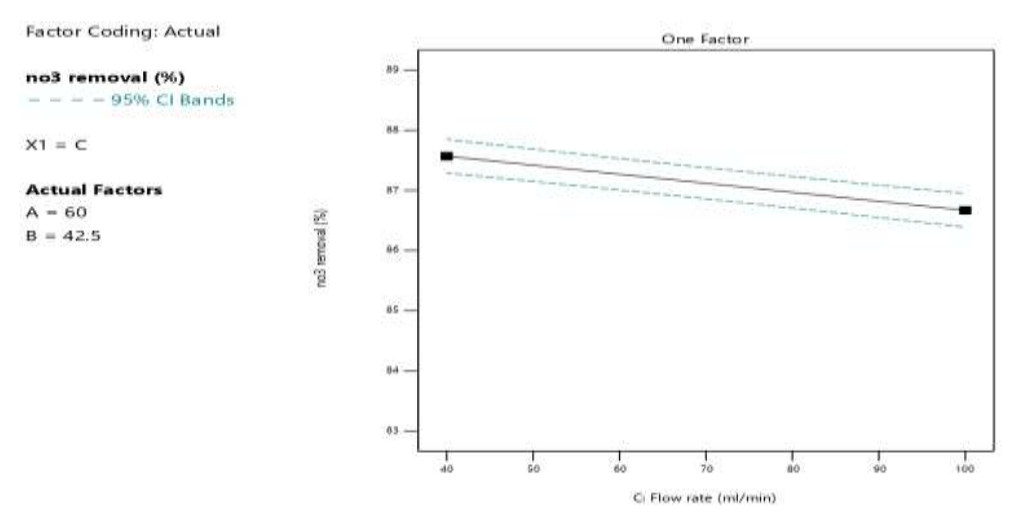


Figure 9. Effect of flow rate on NO₃⁻ Removal.

4.1.6. Effect of temperture on No3- removal after regeneration

Figure 10 displays the effect of temperature on NO₃⁻ removal efficiency after regeneration. The figure indicates that as temperature increases, the removal efficiency also improves. This positive trend suggests that higher temperatures enhance the adsorption kinetics and promote better diffusion of NO₃⁻ ions to the active sites of the regenerated adsorbent. At lower temperatures, the efficiency is reduced, likely due to slower molecular movement and limited interaction with the adsorbent surface. Overall, the figure highlights that elevated temperatures can help compensate for the slight loss in adsorbent performance after regeneration, leading to more effective NO₃⁻ removal.

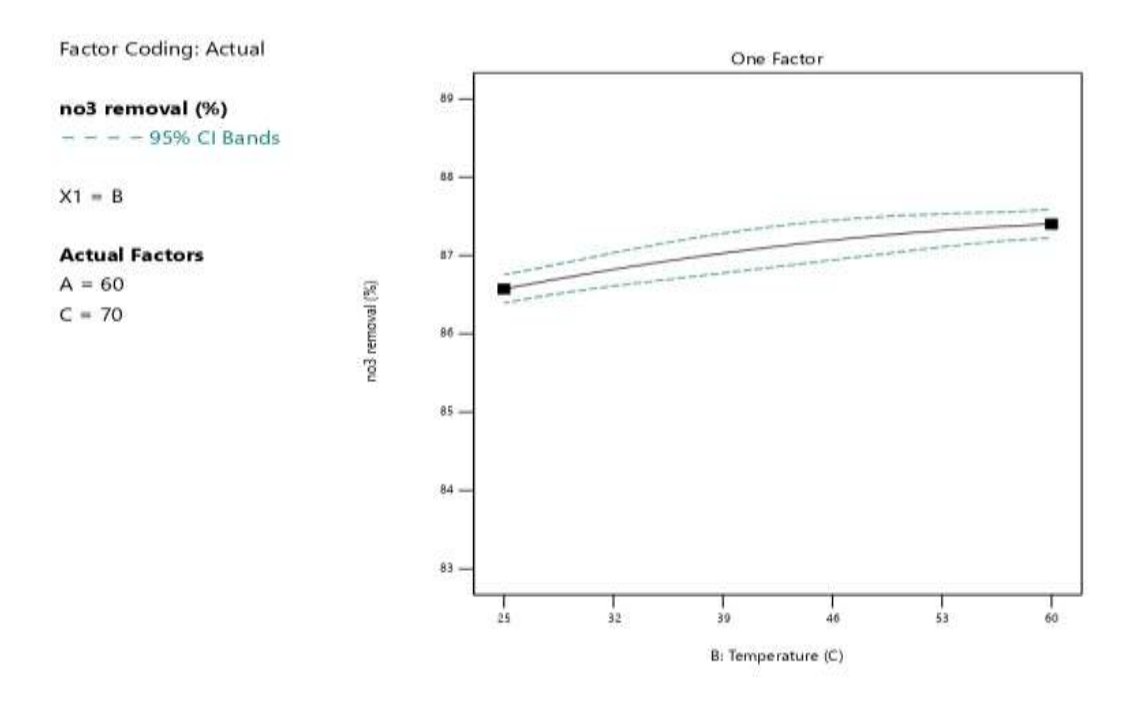


Figure 10. Effect of Temperture on No3- removal after regeneration.

4.2. Effect of Operating Parameters on Pb+2 Removal Efficiency

4.2.1. Interaction Effect Between Concentration and Temperature on Pb+2 Removal

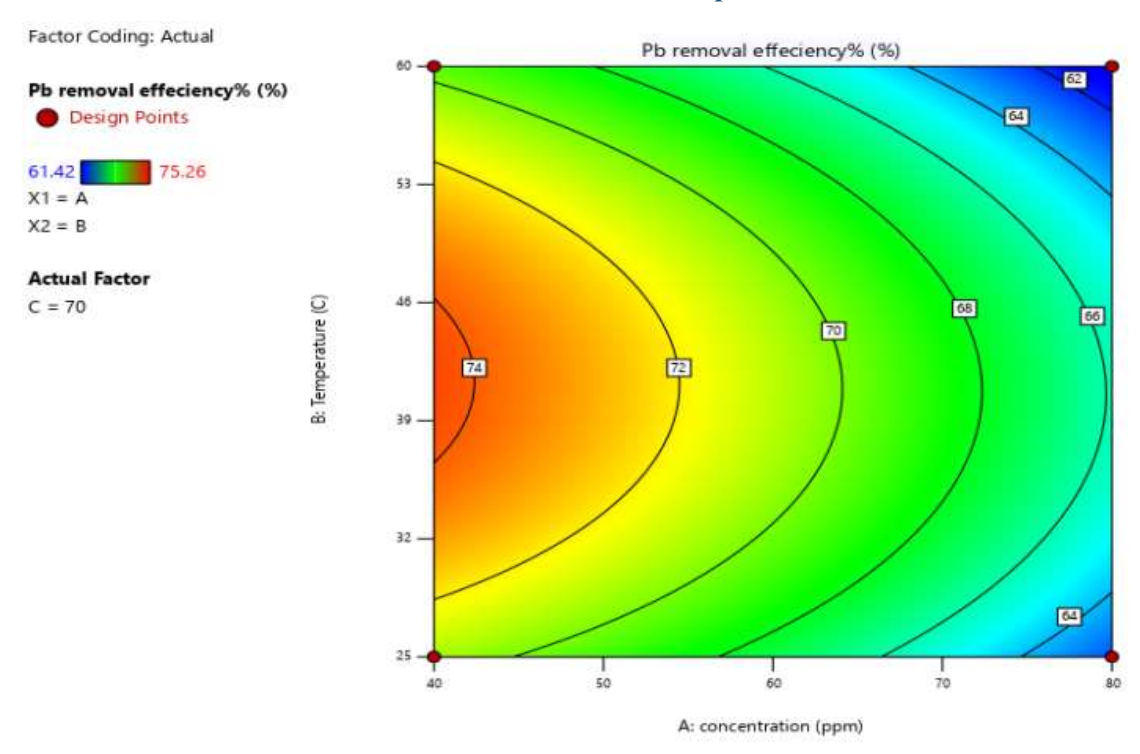


Figure 11. Interaction effect between concentration and temperature on Pb+2 Removal.

Figure 11 illustrates the interaction effect between initial concentration and temperature on Pb²⁺ removal efficiency. The figure shows that at lower concentrations, Pb²⁺ removal remains relatively high regardless of temperature. However, as concentration increases, temperature plays a more significant role higher temperatures lead to improved removal efficiency. This suggests that at elevated concentrations, increased temperature enhances the mobility of Pb²⁺ ions and improves the adsorption capacity of the material. The

interaction indicates a synergistic effect where temperature can partially offset the negative impact of high Pb²⁺ concentrations, emphasizing the importance of thermal conditions in optimizing heavy metal removal.

4.2.2. Interaction Effect Between Concentration and Flow Rate on Pb+2 Removal

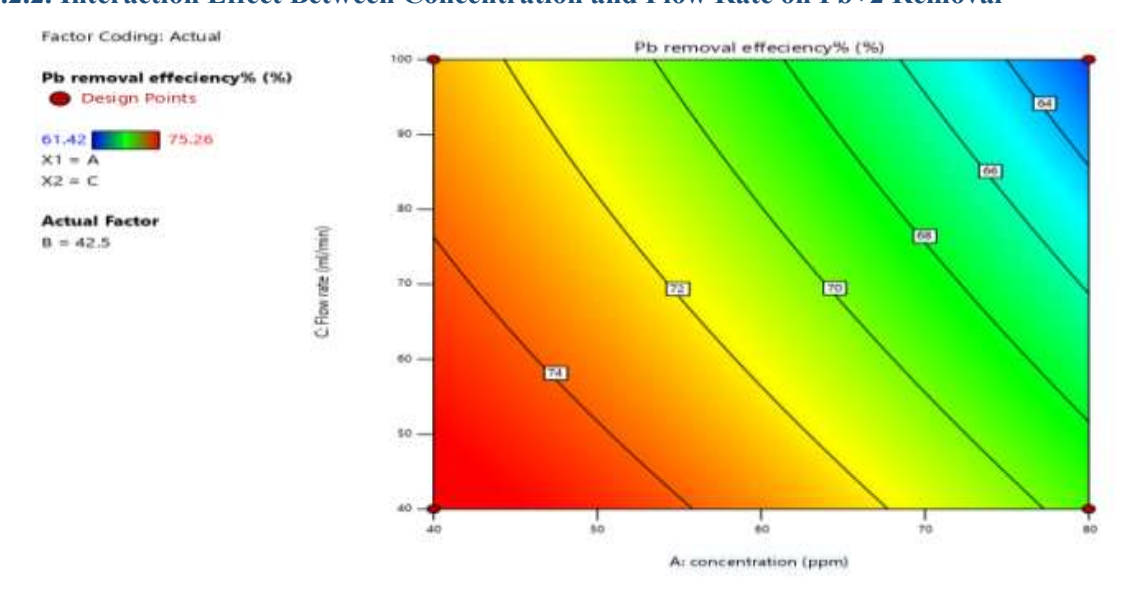


Figure 12. Interaction effect between concentration and flow rate on Pb+2 Removal.

Figure 12 presents the interaction effect between initial concentration and flow rate on Pb²⁺ removal efficiency. The figure shows that at low flow rates, Pb²⁺ removal remains relatively high across varying concentrations due to sufficient contact time between the solution and the adsorbent. However, at higher flow rates, the removal efficiency decreases, particularly at elevated concentrations. This trend suggests that higher concentrations require more time for effective adsorption, which is not achieved at faster flow rates. The interaction highlights that both high concentration and high flow rate negatively impact Pb²⁺ removal, stressing the need to optimize these parameters to maintain effective performance.

4.2.3. Interaction Effect Between Flow Rate and Temperature on Pb+2 Removal

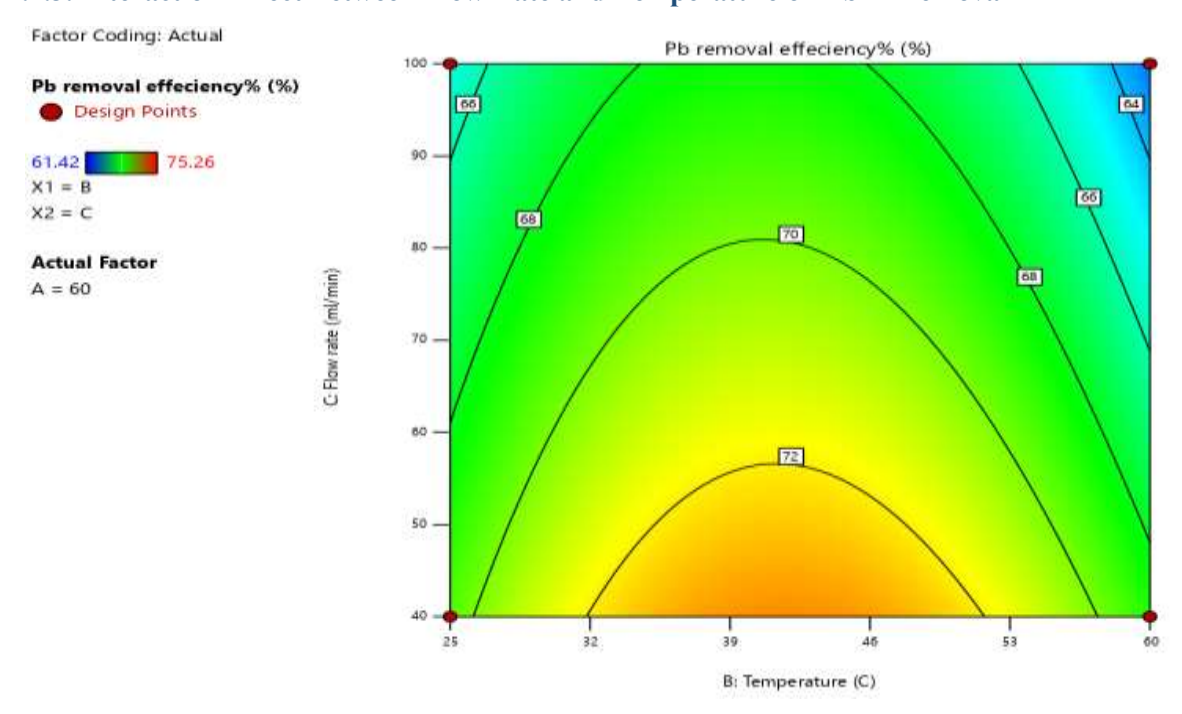


Figure 13. Interaction effect between flow rate and temperature on Pb Removal.

Figure 13 illustrates the interaction effect between flow rate and temperature on Pb²⁺ removal efficiency. The results show that at low flow rates, Pb²⁺ removal remains relatively high across different temperatures, indicating sufficient contact time for effective adsorption. However, at higher flow rates, removal efficiency decreases, particularly at lower temperatures, due to reduced residence time and slower ion mobility. As temperature increases, the negative effect of high flow rate is partially mitigated, suggesting that elevated temperatures enhance adsorption kinetics. This interaction highlights that optimal Pb²⁺ removal after regeneration is achieved at high temperatures and low flow rates.

4.2.4. Effect of Concentration on Pb+2 Removal Efficiency after Regeneration

Figure 14 illustrates the effect of initial concentration on Pb²⁺ removal efficiency after regeneration. The figure shows a clear decline in removal efficiency as the concentration increases. At lower concentrations, the regenerated adsorbent maintains relatively high performance, indicating that the available active sites are sufficient for effective Pb²⁺ adsorption. However, at higher concentrations, the efficiency drops significantly, likely due to saturation of adsorption sites and incomplete regeneration of the material. This trend suggests that the regenerated adsorbent is more effective at treating low-concentration solutions and may require improved regeneration methods or more frequent replacement when treating higher contaminant loads.

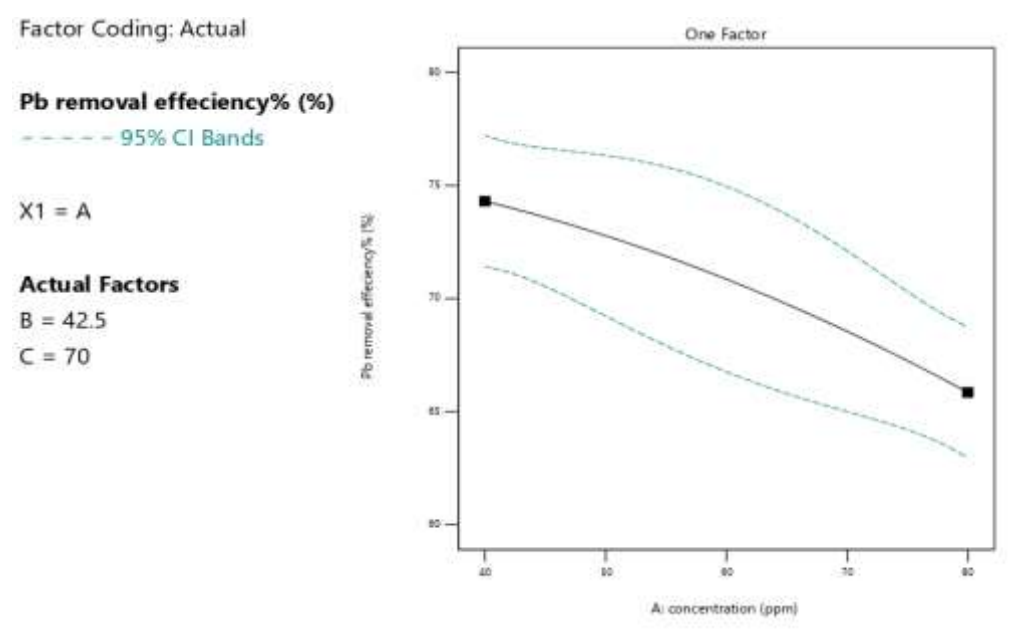


Figure 14. Effect of Concentration on Pb+2 removal efficiency.

4.2.5. Effect of Temperature on Pb+2 Removal Efficiency after Regeneration

Figure 15 illustrates the effect of temperature on Pb²⁺ removal efficiency after regeneration. The graph shows that as temperature increases; the removal efficiency also improves. At lower temperatures, the performance of the regenerated adsorbent is limited, likely due to reduced ion mobility and slower adsorption kinetics. In contrast, higher temperatures enhance the diffusion of Pb²⁺ ions and activate more adsorption sites, leading to better removal efficiency. This trend indicates that operating at elevated temperatures can significantly improve the performance of regenerated adsorbents, helping to maintain effective Pb²⁺ removal across multiple regeneration cycles.

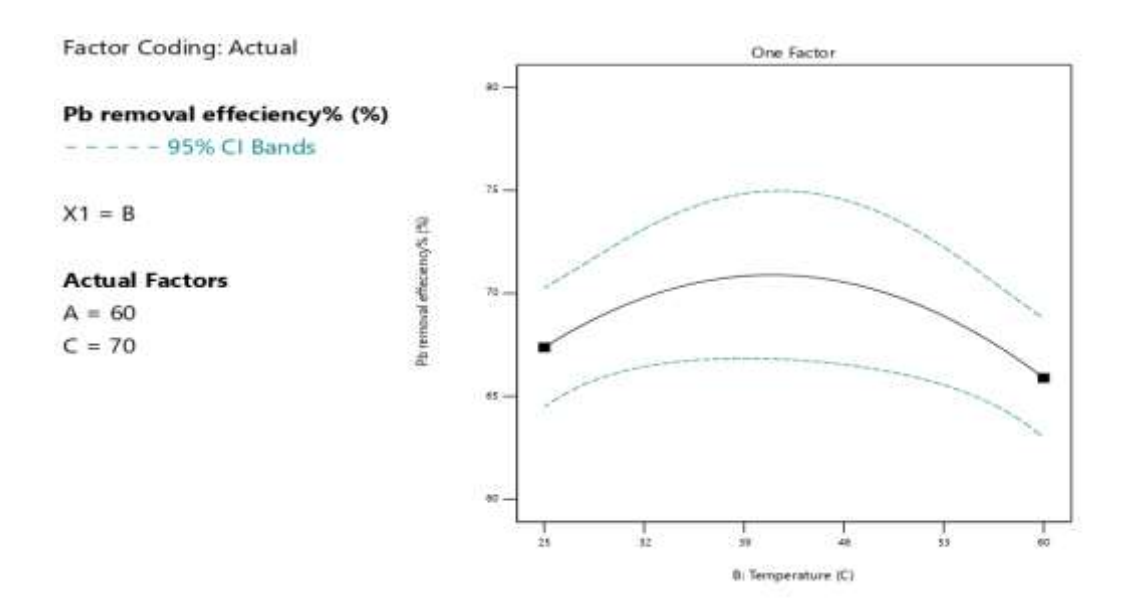


Figure 15. Effect of Temperature on Pb+2 removal efficiency.

4.2.6. Effect of flow rate on Pb+2 Removal Efficiency after Regeneration

Figure 16 illustrates the effect of flow rate on Pb²⁺ removal efficiency after regeneration. The figure shows a clear decreasing trend in removal efficiency as the flow rate increases. At lower flow rates, the regenerated adsorbent performs more effectively, likely due to longer contact time between the Pb²⁺ ions and the adsorption sites, allowing for better uptake. However, as the flow rate increases, the contact time is reduced, leading to insufficient adsorption and lower removal efficiency. This trend emphasizes the importance of maintaining a slower flow rate when using regenerated adsorbents to ensure optimal Pb²⁺ removal performance.

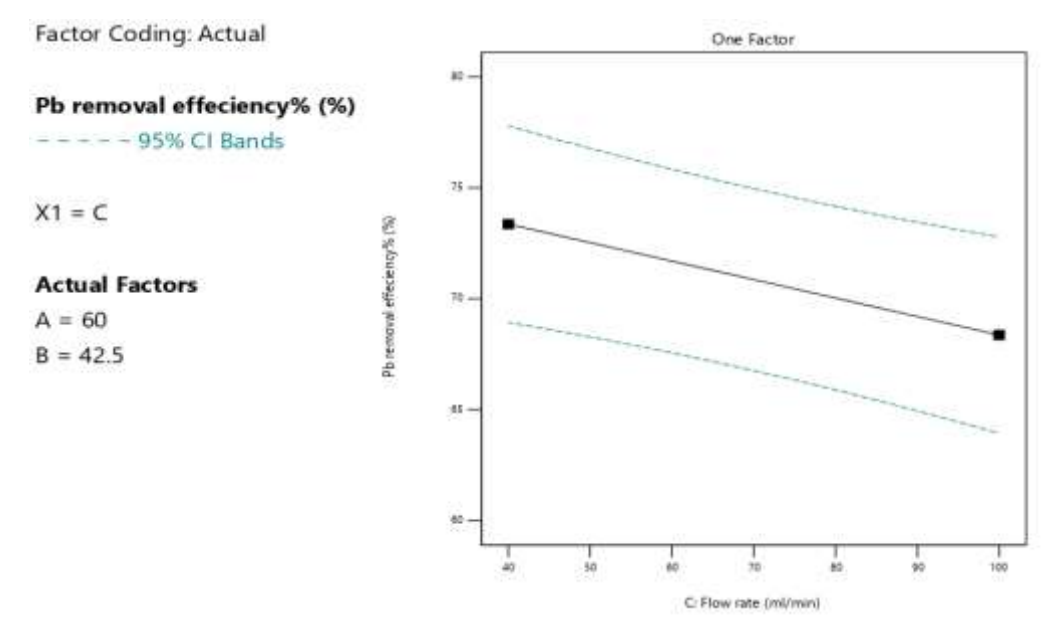


Figure 16. Effect of flow rate on Pb+2 removal efficiency.

4.3. Statistical Results

Experimental data analyzed using Design Expert Software (Version 12) are shown in **Table 3**. ANOVA results (**Tables 4 and 5**) confirm that the quadratic response surface models for nitrate (NO_3^-) and lead (Pb^{2+}) removal are statistically significant (p < 0.05) and reliable. The models demonstrate excellent predictive

accuracy, with high adjusted R² values of 0.9990 for NO₃⁻ and 0.9734 for Pb²⁺. These models effectively support optimization of removal efficiencies.

4.3.1. ANOVA for Quadratic model (Aliased) For No3-

Table 4. Represents No3- removal efficiency.

Source	Sum of Squares	df	Mean Square	F-value	p-value	-
Model	27.30	8	3.41	385.58	0.0002	significant
A-concentration	17.29	1	17.29	1953.36	< 0.0001	
B-Temperature	1.38	1	1.38	155.68	0.0011	
C-Flow rate	1.62	1	1.62	183.05	0.0009	
AB	0.0000	1	0.0000	0.0028	0.9610	
AC	0.0600	1	0.0600	6.78	0.0801	
BC	0.5550	1	0.5550	62.71	0.0042	
A^2	5.18	1	5.18	585.79	0.0002	
B^2	0.0338	1	0.0338	3.82	0.1457	
C^2	0.0000	0				
Residual	0.0266	3	0.0089			
Cor Total	27.33	11				

Factor coding is Coded.

Sum of squares is Type III - Partial

The Model F-value of 385.58 implies the model is significant. There is only a 0.02% chance that an F-value this large could occur due to noise.

P-values less than 0.0500 indicate model terms are significant. In this case A, B, C, BC, A² are significant model terms. Values greater than 0.1000 indicate the model terms are not significant. If there are many insignificant model terms (not counting those required to support hierarchy), model reduction may improve your model.

Final Equation in Terms of Coded Factors

=	NO ₃ ⁻ Removal
	+87.12
*A	-1.47
*B	+0.4150
*C	-0.4500
*AB	-0.0025
*AC	+0.1225
*BC	-0.3725
*A ²	-1.61

-0.1300 *B² +0.0000 *C²

The equation in terms of coded factors can be used to make predictions about the response for given levels of each factor. By default, the high levels of the factors are coded as +1 and the low levels are coded as -1. The coded equation is useful for identifying the relative impact of the factors by comparing the factor coefficients.

4.3.2. ANOVA for Quadratic model (Aliased) For Pb+2

Table 5. Represents Pb+2 removal efficiency.

Source	Sum of Squares	df	Mean Square	F-value	p-value	
Model	242.98	8	30.37	13.71	0.0272	significant
A-concentration	143.14	1	143.14	64.61	0.0040	
B-Temperature	4.40	1	4.40	1.98	0.2537	
C-Flow rate	49.95	1	49.95	22.55	0.0177	
AB	0.1560	1	0.1560	0.0704	0.8079	
AC	4.10	1	4.10	1.85	0.2669	
BC	0.6084	1	0.6084	0.2746	0.6365	
A^2	1.22	1	1.22	0.5527	0.5111	
B^2	35.87	1	35.87	16.19	0.0276	
C^2	0.0000	0				
Residual	6.65	3	2.22			
Cor Total	249.62	11				

Factor coding is Coded.

Sum of squares is Type III - Partial

The Model F-value of 13.71 implies the model is significant. There is only a 2.72% chance that an F-value this large could occur due to noise.

P-values less than 0.0500 indicate model terms are significant. In this case A, C, B² are significant model terms. Values greater than 0.1000 indicate the model terms are not significant. If there are many insignificant model terms (not counting those required to support hierarchy), model reduction may improve your model.

Final Equation in Terms of Coded Factors

Pb ⁺² Removal Efficiency%	=
+70.87	
-4.23	*A
-0.7413	*B
-2.50	*C
-0.1975	*AB
-1.01	*AC

-0.3900	*BC
-0.7825	*A ²
-4.24	*B ²
+0.0000	*C ²

The equation in terms of coded factors can be used to make predictions about the response for given levels of each factor. By default, the high levels of the factors are coded as +1 and the low levels are coded as -1. The coded equation is useful for identifying the relative impact of the factors by comparing the factor coefficients.

4.4. Experiment design

Under the defined experimental setup, optimal operating conditions were established to enhance ion-exchange performance. A lead nitrate feed of 40.45 mg L⁻¹ was treated at pH 7.0 \pm 0.1, temperature 42.8 °C, and flow 60 mL min⁻¹. Two fixed-bed columns (40 g resin each) were arranged in series: a strong-acid cation exchanger (Pure lite C100) targeting Pb²⁺ and a strong-base anion exchanger (ResinexTM NR-1) targeting NO₃⁻. Durability and reusability were evaluated over six regeneration cycles; each cycle comprised 15 min of service, regeneration with 10 % (w/w) NaCl. Cycle 1 was defined as the baseline, achieving removal efficiencies of 82.5 % for Pb²⁺ and 92.3 % for NO₃⁻; subsequent cycles are reported relative to this baseline. A gradual decline in performance was observed with repeated reuse, consistent with incomplete desorption and partial occupation of high-affinity sites: Cycle 2 Pb²⁺ 80.9 %, NO₃⁻ 91.5 %; Cycle 3 Pb²⁺ 78.6 %, NO₃⁻ 89.8 %; Cycle 4 Pb²⁺ 76.3 %, NO₃⁻ 88.2 %; Cycle 5 Pb²⁺ 72.9 %, NO₃⁻ 85.2 %; Cycle 6—Pb²⁺ 70.2 %, NO₃⁻ 83.6 % as shown in **Figure 17**. Overall retention at Cycle 6 remained high≈ 85 % of the Cycle 1 level for Pb²⁺ and ≈ 91 % for NO₃⁻ indicating that the applied brine protocol sustained robust functionality across multiple regenerations, with the anion resin exhibiting a slower efficiency decay than the cation resin under identical conditions. both resins demonstrated good reusability, though further optimization of regeneration conditions is recommended for sustained efficiency^[20].

The findings confirm that 10% NaCl is effective for short-term regeneration, allowing Pure lite C100 and Resinex NR-1 to sustain satisfactory performance under continuous flow with periodic regeneration. However, the gradual decline in removal efficiency suggests that for extended or industrial use, the regeneration process requires enhancement. Potential improvements include extending the contact time with the regenerant, increasing NaCl concentration, or implementing occasional deep-cleaning procedures with alternative chemicals to better restore resin functionality^[21,22]. In summary, the ion exchange system showed excellent initial removal efficiency and maintained stable regeneration performance across four cycles, with no signs of fouling or flow obstruction. The results validate that the combination of Pure lite C100 and Resinex NR-1 resins, under optimized operational conditions of flow rate, temperature, and pH, can consistently and effectively remove Pb²⁺ and NO₃- from aqueous solutions.

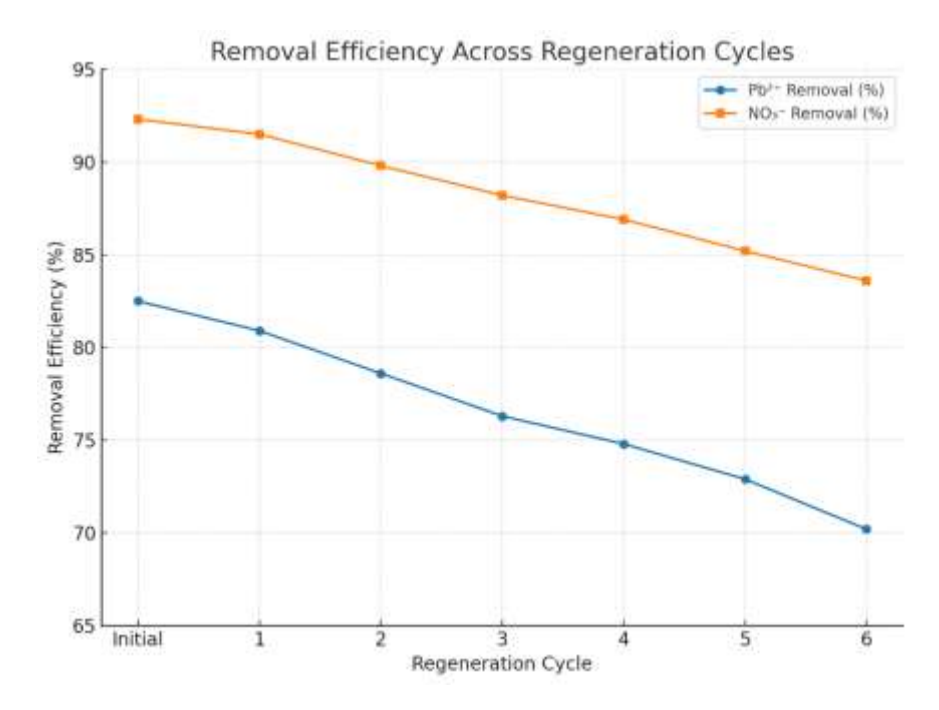


Figure 17. Removal efficiency across six regeneration cycles.

5. Conclusion

Operating a continuous dual fixed-bed system (Purelite C100, ResinexTM NR-1) at neutral pH with 40 g per column achieved high initial removals 82.5% for Pb²⁺ and 92.3% for NO₃⁻ under optimized conditions (43 °C, 60 mL min⁻¹, 40 mg L⁻¹). Across six regenerations with 10% NaCl, performance declined moderately to 70.2% (Pb²⁺) and 83.6% (NO₃⁻), indicating good reusability, with the cation bed more regeneration-sensitive due to stronger Pb²⁺ binding. Response-surface/ANOVA results confirmed well-fitting quadratic models and identified inlet concentration and flow rate as the dominant negative drivers via contact-time limitations, while elevated temperature improved kinetics and partially offset high-load effects. Overall, a 10% NaCl protocol is an effective, practical baseline for routine operation; capacity retention can be further sustained by extending regenerant—bed contact time, incorporating occasional intensified (deep-clean) steps, or applying condition-based adjustments to regenerant strength/volume. For scale-up, operating at moderate concentration and flow with elevated temperature and adopting condition-based regeneration is recommended, with future work comparing counter-current versus co-current modes and exploring hybrid regenerants to enhance Pb²⁺ desorption.

Conflict of interest

The authors declare no conflict of interest.

References

- A. Q. Jasim and S. K. Ajjam, "Removal of heavy metal ions from wastewater using ion exchange resin in a batch process with kinetic isotherm," South African J. Chem. Eng., vol. 49, no. March, pp. 43–54, 2024, doi: 10.1016/j.sajce.2024.04.002.
- 2. N. M. Marin, M. Nita Lazar, M. Popa, T. Galaon, and L. F. Pascu, "Current Trends in Development and Use of Polymeric Ion-Exchange Resins in Wastewater Treatment," Materials (Basel)., vol. 17, no. 23, pp. 1–19, 2024, doi: 10.3390/ma17235994.
- 3. M. S. Ummah, No 主観的健康感を中心とした在宅高齢者における健康関連指標に関する共分散構造分析 Title, vol. 11, no. 1. 2019. [Online]. Available: http://scioteca.caf.com/bitstream/handle/123456789/1091/RED2017-Eng-8ene.pdf?sequence=12&isAllowed=y%0Ahttp://dx.doi.org/10.1016/j.regsciurbeco.2008.06.005%0Ahttps://www.researchgate.net/publication/305320484_SISTEM_PEMBETUNGAN_TERPUSAT_STRATEGI_MELESTARI

- 4. R. Adolph, "済無 No Title No Title No Title," pp. 1–23, 2016.
- S. K. Sharma and R. Sanghi, Advances in water treatment and pollution prevention, vol. 9789400742. 2012. doi: 10.1007/978-94-007-4204-8.
- 6. C. Charcosset, "Classical and Recent Developments of Membrane Processes for Desalination and Natural Water Treatment," Membranes (Basel)., vol. 12, no. 3, pp. 1–28, 2022, doi: 10.3390/membranes12030267.
- 7. J. B. de Heredia, J. R. Domínguez, Y. Cano, and I. Jiménez, "Nitrate removal from groundwater using Amberlite IRN-78: Modelling the system," Appl. Surf. Sci., vol. 252, no. 17, pp. 6031–6035, 2006, doi: 10.1016/j.apsusc.2005.11.030.
- 8. M. J. McCoy, "Ion exchange," Ultrapure Water, vol. 13, no. 1, pp. 20–31, 1996, doi: 10.1201/noe0824727857.ch185.
- 9. S. Kumar and S. Jain, "History, introduction, and kinetics of ion exchange materials," J. Chem., vol. 2013, 2013, doi: 10.1155/2013/957647.
- 10. G. P. Ponnaiah, S. Lakshmi, A. B. L. S. Sivalingam, and S. Sivalingam, "A review of current practices on lead ions removal from different aqueous streams," Brazilian J. Dev., vol. 10, no. 3, p. e68334, 2024, doi: 10.34117/bjdv10n3-062.
- 11. T. E. Bulletin, "Purolite C100 Sodium Cycle".
- 12. P. D. Sheet, P. Applications, R. Approvals, T. Packaging, and T. Physical, "Purolite TM C100," pp. 3–5, 2025.
- 13. T. Properties, T. Applications, S. D. Conditions, S. Packaging, and K. Features, "Resinex-RX-AP-Strong-base-anion-exchange-resin-Lenntech".
- 14. LENNTECH, "Resinex NR-1," 2014.
- 15. S. Al-Asheh and A. Aidan, "A Comprehensive Method of Ion Exchange Resins Regeneration and Its Optimization for Water Treatment," Promis. Tech. Wastewater Treat. Water Qual. Assess., 2021, doi: 10.5772/intechopen.93429.
- 16. A. A. Hekmatzadeh, A. Karimi-Jashani, N. Talebbeydokhti, and B. Kløve, "Modeling of nitrate removal for ion exchange resin in batch and fixed bed experiments," Desalination, vol. 284, pp. 22–31, 2012, doi: 10.1016/j.desal.2011.08.033.
- 17. K. J. H. and G. T. John C. Crittenden, R. Rhodes Trussell, David W. Hand, "Ion Exchange: MWH's Water Treatment: Principles and Design, Third Edition John," John Wiley Sons, Inc, 2012.
- 18. S. L. Gromov and A. A. Panteleev, "Counterflow ionite regeneration technologies for water treatment: Part 1," Therm. Eng., vol. 53, no. 8, pp. 620–625, 2006, doi: 10.1134/S0040601506080076.
- 19. A. M. Wachinski, Environmental Ion Exchange: Principles and Design, Second Edition. 2016. doi: 10.1201/9781315368542.
- R. B. Gauntlett, "Nitrate removal from water by ion exchange," Water Treatm. Exam., vol. 24, no. 3 pt 3, pp. 172–193, 1AD, doi: 10.17508/cifst.2017.9.2.15.
- 21. R. R. Yaragal and S. Mutnuri, "Nitrates removal using ion exchange resin: batch, continuous column and pilot-scale studies," Int. J. Environ. Sci. Technol., vol. 20, no. 1, pp. 739–754, 2023, doi: 10.1007/s13762-021-03836-8.
- 22. A. Lalmi, K. E. Bouhidel, B. Sahraoui, and C. el H. Anfif, "Removal of lead from polluted waters using ion exchange resin with Ca(NO3)2 for elution," Hydrometallurgy, vol. 178, no. 2017, pp. 287–293, 2018, doi: 10.1016/j.hydromet.2018.05.009.
- 23. Purolite, "Ion Exchange Resin Regeneration and Cleaning," Purolite, [Online]. Available: https://www.purolite.com/index/core-technologies/industry/food-and-beverage/sugar-refining-applications/cane-sugar-production/ion-exchange-resin-regeneration-and-cleaning. [Accessed: 17-Aug-2025].
- 24. Veolia Water Technologies, "Chapter 08 Ion Exchange," Ion Exchange Handbook, [Online]. Available: https://www.watertechnologies.com/handbook/chapter-08-ion-exchange. [Accessed: 17-Aug-2025].
- 25. D. Carlson, "Resin Regeneration Fundamentals," WaterWorld Magazine, 2018. [Online]. Available: https://www.waterworld.com/residential-commercial/article/14307808/resin-regeneration-fundamentals. [Accessed: 17-Aug-2025].
- 26. Wikipedia, "Ion Exchange," Wikipedia, 2025. [Online]. Available: https://en.wikipedia.org/wiki/Ion_exchange. [Accessed: 17-Aug-2025].